Thermotropic Polyester Amide-Carbon Fiber Composites

TAI-SHUNG CHUNG and PAUL E. McMAHON, *Celanese Specialties Operation, 86 Morris Avenue, Summit, New Jersey 07901*

Synopsis

Liquid crystal polymers (LCP) have been developed for the first time as a thermoplastic matrix for high-performance composites. A successful melt impregnation method has been developed that results in the production of continuous carbon fiber (CF)-reinforced LCP prepreg tape. Subsequent layup and molding of prepreg into laminates has yielded composites of good quality.

Tensile and flexural properties of LCP-CF composites are comparable to those of epoxy-CF composites. LCP-CF composites have better impact resistance than the latter, although epoxy-CF composites possess superior compression and shear strength. LCP-CF composites have good property retention until 200°F (67% of room temperature value). Above 200°F, mechanical properties are found to decrease significantly. Experimental results indicate that the poor compression and shear strength may be due to the poor interfacial adhesion between the matrix and carbon fiber.

INTRODUCTION

The interest in thermoplastic carbon fiber (CF) composites for the aircraft and aerospace industry is rapidly growing. Thermoplastic materials are more ductile and consequently have higher toughness and impact resistance than their thermoset counterparts. Thermoplastics also offer significant process advantages, such as unlimited shelf life and formability when heated which should result in lower fabrication costs. However, since most thermoplastics have much higher melt viscosity than thermosets, the fabrication process and impregnation mechanism for the two systems are quite different.

In recent years, Celanese has developed a new class of polymeric material based on hydroxynaphthoic acid chemistry, consisting of rigid backbone molecules. These polymers exhibit liquid crystalline order in the melt that produces a high degree of molecular orientation and excellent mechanical properties. Unlike lyotropic liquid crystal polymers, these thermotropic liquid crystal polymers (LCP) can be easily processed using conventional injection molding, extrusion, and melt spinning equipment. The melting point of Celanese LCP materials is highly dependent on the monomer composition of the polymer as well as the polymerization conditions.

Articles fabricated from LCP materials have shown mechanical properties generally superior to conventional fiber-reinforced engineering resins. Solvent resistance as well as dimensioal stability are also generally superior to conventional thermoplastic resins. Due to the unique mechanical prop-

Journal of Applied Polymer Science, Vol. 31, 965–977 (1986)
 CCC 0021-8995/86/040965-13$04.00

erties and excellent chemical resistance, it is anticipated that these LCP materials may possibly offer advantages as a thermoplastic matrix resin. Work related to fabrication techniques and mechanical properties of LCP-carbon fiber composites is documented in this report.

LITERATURE SURVEY

Development of thermoplastic-continuous cabon fiber composites began about a decade ago. Hoggatt investigated polysulfone and phenoxy polymers.[1] Hartness and coworkers studied polyphenylene sulfide (PPS), polyphenylene sulfone, and polyether ether ketone (PEEK) matrices.[2-5] McMahon and Maximovich developed and evaluated Nylon 6,6 and polybutylene terephthalate (PBT) matrices.[6] The effects of various surface finishes on composite performance have been discussed. Sheppard and House evaluated polyimide-capped polysulfone, PPS, polyamide-imide, PEEK, and PBT.[7] More detailed studies of PEEK matrix composites were also reported in the recent literature.[8-11]

In 1976, a new class of materials with excellent chemical resistance and mechanical strength was developed by researchers at Tennessee Eastman.[12-14] The extraordinary change in the properties of these thermoplastics can be explained through the physical formation of liquid crystals in the melt. Since then, a variety of liquid crystal-containing polymers have been invented.[15-23] Because of their lower melt viscosity, they flow easier and offer processing advantages over conventional thermoplastics. Studies of LCP can be generally divided into two catagories: (1) formation and chemical structure of LCP, and (2) rheologic phenomena.

Smith[24] compared the basic differences between low-molecular-weight liquid crystals and LCP. He summarized the orientation behavior and physical properties of LCP from previous reviews and literature. White and Fellers[25] reviewed the formation and chemical structure of macromolecular liquid crystals that form fibers with unusally high levels of orientation and strength. Lenz and his coworkers[26,27] gave a thorough review of the previous studies on the synthesis of thermotropic liquid crystalline polyesters. They discussed and investigated the advantages of using flexible, semiflexible, and nonmesogenic spacer groups in LCP for suppressing the melting points below their decomposition temperatures. Jackson[28] also studied the effect of polymer structure on the melting points and mechanical properties of liquid crystalline aromatic polyesters. Krigbaum et al.[29] investigated the effect of the number of methylene units in thermotropic polyesters. Calundann and Jaffe[30] traced the industrial developments of anisotropic polymers through their theoretical origins to synthesis and on to fabrications of fiber, film, and molded products. The effects of polymer composition on melting temperatures, processibilities, and mechanical properties of fiber have been discussed in detail.

The rheology of LCP was reviewed by Porter and Johnson[31] in 1967, and then by Baird in 1978.[32] Recently, Wissbrun[33] gave a more in-depth and thorough review of this subject based on the three-region flow curve proposed by Onogi and Asada.[34] In general, the viscosity of LCP is much lower

than that of conventional polymers at a comparable molecular weight. The relaxation time and elasticity of LCP are greater than those of isotropic polymers. In addition, LCP often show a variety of phenomena that are not seen with isotropic polymers. These include the observation of negative first normal stress difference,[35,36] regions of shear thickening viscosity, and the secondary maximum in transient shear flow.[37,38]

MATRIX CHARACTERISTICS

Polymer Formation and Melt Characterization

The polymer used in these studies is an all aromatic copolyester of 2,6-hydroxynaphthoic acid, terephthalic acid, and 4'-hydroxy-acetanilide. This polymer was invented by East et al., and the details of polymerization conditions were described in the patent.[39] The polymer is a high-molecular-weight copolyester and exhibits ordered structure in the melt, as indicated by birefringent optical properties. Figure 1 demonstrates that it melts at about 280–285°C as determined by differential scanning calorimetry using a 20°C/min heatup rate. The polymer has an inherent viscosity of approximately 4.5 dL/g. Figure 2 shows the melt viscosity as a function of shear rate and temperature. This polymer has much lower viscosity than most of the conventional thermoplastic polymers.

Polymer Tensile Properties and Chemical Resistance

The tensile properties of the neat resin under different environmental conditions are shown in Table I. The chemical resistance to Skydrol and methylene chloride is excellent.

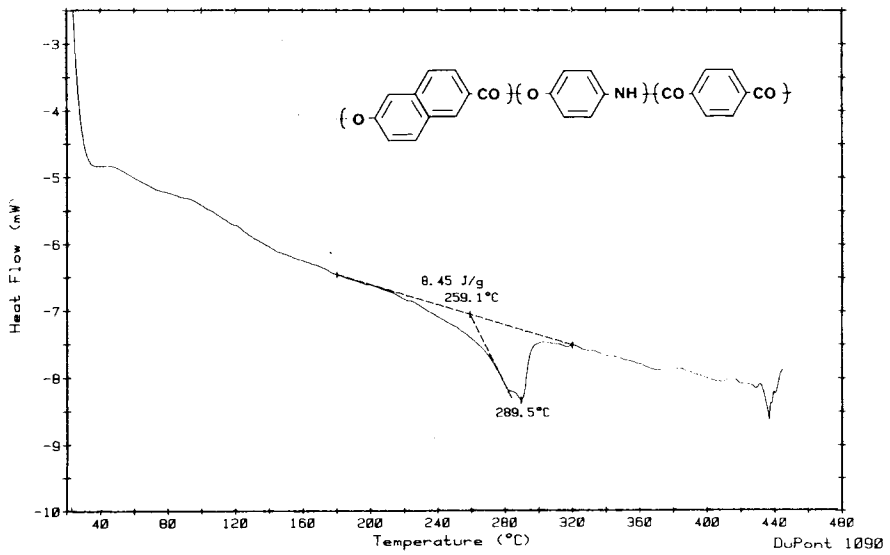

Fig. 1. The DSC curve of a LCP film.

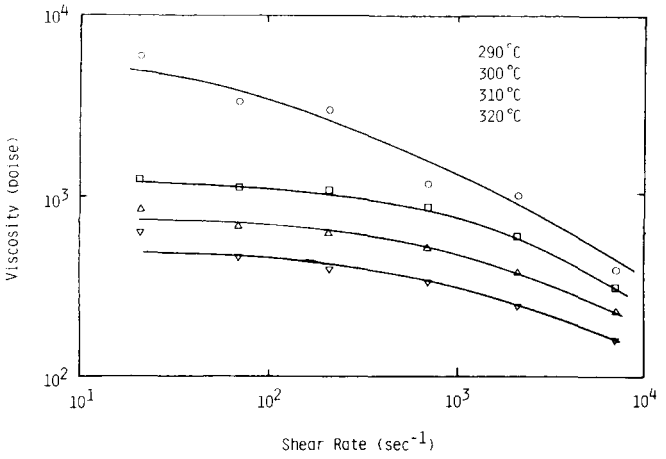

Fig. 2. Viscosity of LCP as a function of shear rate and temperature.

Dynamic mechanical analyses of as-extruded strands were conducted at temperatures ranging from −120°C to 280°C. Figure 3 shows the results and indicates that the modulus is highest at cryogenic conditions, but it drops sharply at both the β transition (70°C) and the α transition (140°C).

Crack Propagation Measurements

The future toughness of neat resin was determined by measuring the mode I fracture toughness K_{Ic} of injection-molded LCP plaques. Because the injection gate was located on the peripheral edge of the molded disk, it produced an anisotropic flow field. Two measurements were made parallel to the machine direction (designated longitudinal) and four in the direction perpendicular to the flow from the gate (designated transverse).

Specimens were fabricated to the geometry specified in Figure 4. Load was introduced into the specimen through 1.27 cm (1/2 in.) pins inserted through a clevis arrangement mounted in a standard TTC Instron test machine. A schematic of the test setup is shown in Figure 5. Load was

TABLE I
Tensile Properties of LCP at Room Temperature

Conditioning	% Weight gain	Tensile Strength (MPa)	(ksi)	Tensile Modulus (GPa)	(msi)
Control	—	162.1	(23.2)	23.5	(3.36)
140°F/98% RH (30 days)	0.036	141.1	(20.2)	22.4	(3.20)
CH_2Cl_2 (30 days)	-0.023	176.8	(25.3)	24.7	(3.53)
Skydrol (30 days)	0.018	174.7	(25.0)	21.0	(3.00)

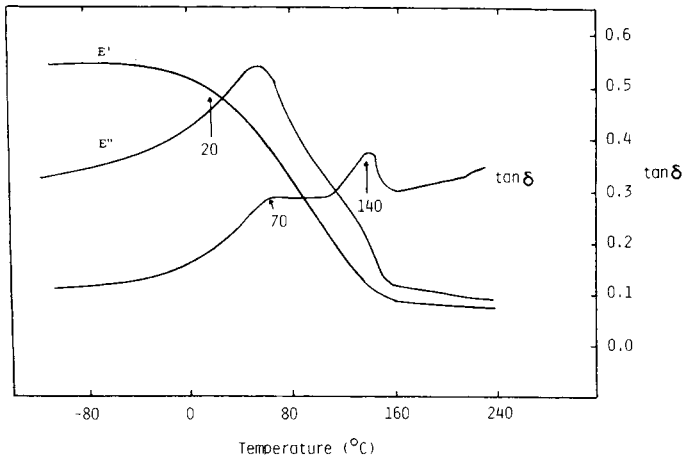

Fig. 3. DMA curve of as-extruded LCP strand.

applied by moving the crosshead at a constant rate of displacement until the crack in the specimen began to propagate as indicated by a drop in load recorded on the load displacement curve. At this point the test was stopped, the specimen unloaded, and a measurement taken of the new crack length. The load at which the crack of length a_i begins to propagate is designated f_i and used to determine $\mathbf{K}_{Ic}$ for that given crack length. Crack lengths of the "natural cracks" were determined by averaging the measured length on each surface of specimen. Natural cracks are defined as cracks whose crack front is the result of a previous propagation event, not a machining operation. The calculation of K_{Ic} employs the relationship[40]

$$K_{Ic} = \frac{f_i}{BW^{1/2}} Y(a_i/W)$$

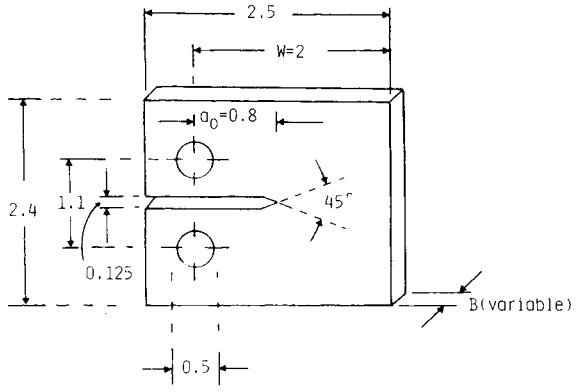

Fig. 4. Compact tension specimen configuration (inches).

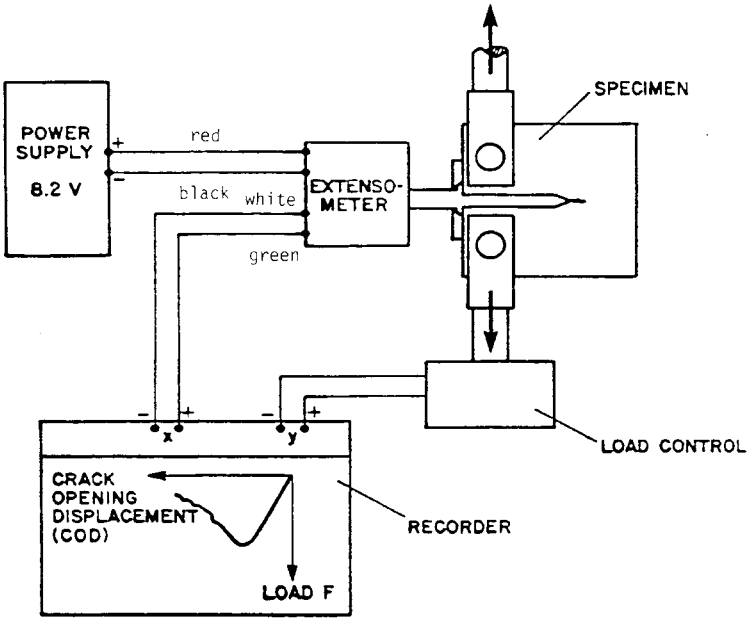

Fig. 5. Block diagram of load-crack opening displacement measurements.

where

$$K_{Ic} = \text{fracture toughness (mode I)}$$

$$f_i = \text{propagation load}$$

$$B = \text{thickness}$$

$$W = \text{width}$$

$$a_i = \text{crack length}$$

$$Y(a_i/W) = \text{geometric correction factor}$$

$$Y(a_i W) = 29.6(a_i/W)^{1/2} - 185.5(a_i/W)^{3/2} + 6.55.7(a_i/W)^{5/2} - 1017(a_i/W)^{7/2} + 638.9(a_i/W)^{9/2}$$

The test procedure is repeated on a single specimen for several crack lengths, usually about four. When the crack gets to within 1.27 cm (0.5 in.) of the specimen's edge, no further data are taken due to the influence of the edge on the measurements. Figure 6 presents the results for longitudinal measurements from specimens labeled L1 and L3. The relatively high scatter is typical for this type of test applied to polymeric and fiber reinforced materials. The solid line indicates the average K_{Ic} determined from natural crack data only, and the dashed line the average K_{Ic} including all data points. For these specimens, the crack propagation was predominantly col-

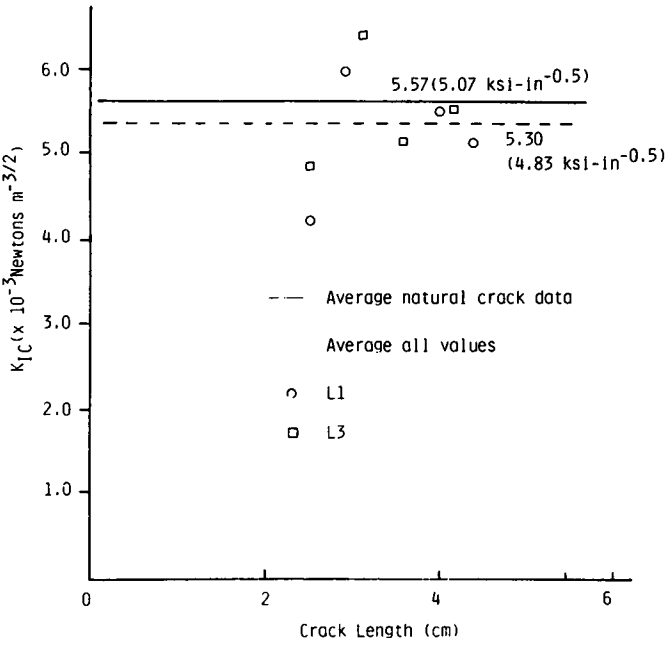

Fig. 6. K_{Ic} versus crack length for longitudinal specimens.

inear with the starter crack but wandered slightly (see Fig. 7). This slight amount of wandering accounts for most of the variability in the data.

Results for the transverse specimens are shown in Figure 8. In these specimens, the crack did not propagate colinearly with the machined crack. A typical crack path is shown in Figure 7. Under these circumstances, the

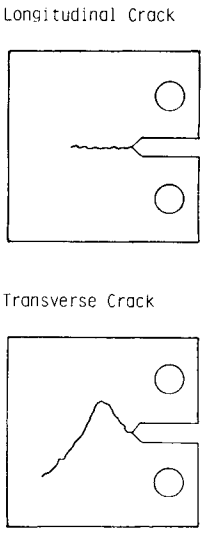

Fig. 7. Crack propagation characteristics for longitudinal and transverse specimens.

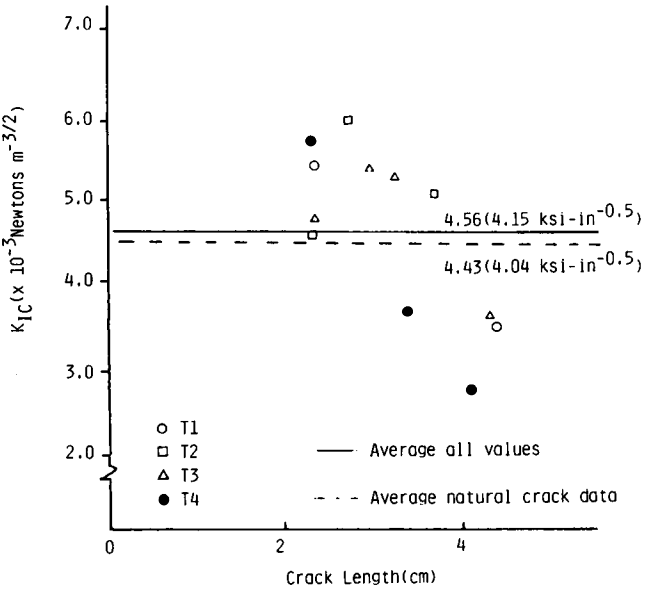

Fig. 8. K_{Ic} versus crack length for transverse specimens.

K_{Ic} calculations are significantly in error. Therefore, the data presented in Figure 8 are not viewed as a valid quantitative measure of K_{Ic} in the transverse direction of the material. Again, the averages are shown based on natural crack data (solid line) and all data (dashed line), but these numbers are probably lower than the actual K_{Ic}.

COMPOSITE FABRICATION PROCESS

Prepreg Line

The impregnation was carried out in a crosshead tape die. Molten LCP polymer was supplied by a twin screw extruder to the channels of the tape die. The extruder has three temperature controllers to monitor the temperature profiles at feeding, transition, and metering zones. In these experiments, these three controllers were set at 290°C. The crosshead die was set at 320°C. Ten to twenty yarns of Celion 6000 carbon fiber could be pulled horizontally through the die at speeds ranging from inches per minute to 10 feet/min. Tapes produced via this process had 40–55 volume% fiber loading, fair wetout, and good fiber alignment. Their thicknesses varied from 0.007 to 0.012 cm. The details of process conditions and fabrication technology have been published by Chung.[41]

Panel Preparation

Carbon fiber-LCP resin composite panels were prepared by compression molding stacked layers of the tape. This compression-molding process utilized a Carver laboratory press, a 50-ton hydraulic press, and a highly

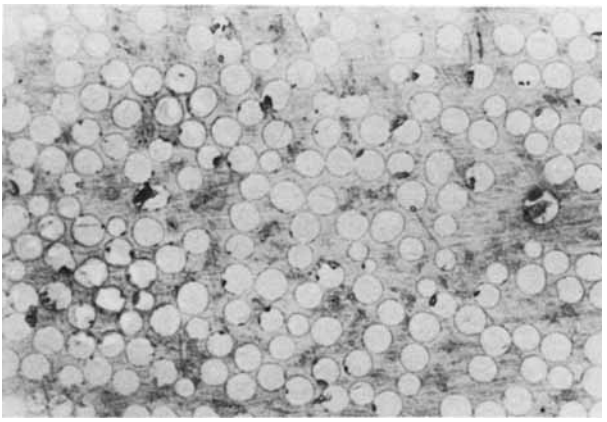

Fig. 9. Scanning electron micrograph of a cross section of LCP carbon fiber composites (57% volume) (× 1000).

polished 8.9 × 26.5 cm rectangular steel mold. Heating elements were installed in the Carver press, and their temperature was monitored by a temperature controller in each platen. The process is therefore capable of molding panels at specific temperature and pressure conditions. The thickness of fabricated panels was controlled by the number of tape layers inserted into the mold for compression molding. The tight tolerances on the mold allowed pressure in excess of 6.9×10^6 N/m^2 with little polymer leakage. Usually, panels were compression molded at 300–340°C under a pressure of $7–35 \times 10^5$ N/m^2 for 10–15 min in the hot Carver press and then transferred to a cold hydraulic press for cooling. The pressure during the cooling stage was about 6.9×10^6 N/m^2.

Vacuum Bag

Minimum void content in composites is essential for maximizing mechanical properties. Without vacuum applied to the layup prior to compression molding, air was trapped between the various plies and caused a greater than desirable void content in the composite panel. By wrappng the ply assembly with a high-temperature-resistant Kapton film and applying vacuum, we successfully reduced void content in the composite panel to < 0.8% by volume (density measurement).

Figure 9 shows a scanning electron micrograph of a cross section of a

TABLE II
Tensile Properties of Unidirectional Composites

CF volume (%)	Conditions	Tensile Strength, MPa (ksi)	Tensile modulus, GPa (msi)	Tensile strain (%)
56.5	Dry	1492 (217)	143 (20.7)	1.045
56.5	Wet	1297 (188)	121 (17.6)	1.071

TABLE III
Flexural Properties of LCP-CF Composites

Fiber content (vol %)	Conditions	Flexural Strength, MPa (ksi)	Flexural Modulus, GPa (ksi)
51	RT (dry)	1515 (220)	106.5 (15.45)
51	RT (wet)	1447 (210)	106.5 (15.39)
51	200°F (dry)	1054 (153)	106.2 (15.42)
51	200°F (wet)	904 (140)	105.3 (15.28)
51	250°F (dry)	744 (108)	98.8 (14.34)
51	250°F (wet)	854 (124)	97.8 (14.19)

compression-molded carbon fiber (Celion 6000, unsized) LCP panel and clearly illustrates a good fiber-resin distribution.

Test Specimen Preparation

The mechanical properties of the molded panel were determined using ASTM methods. Specimens were prepared with 0° carbon fiber orientation. Flexural strength and modulus were measured using a three-point flex test and approximately 32:1 span-depth ratio; short beam shear strength used a 4:1 span-depth ratio. Compression properties were measured using the compression fixture and procedure described in ASTM D3410, where test specimens were 0.20 cm thick, 0.635 cm wide, and 10.8 cm long. Tensile specimens were 1.27 cm wide and 21.59 cm long. Four fiberglass tabs, 1.27 cm wide and 5.72 cm long, were mounted on specimens prior to testing. Tensile strength samples of 45° were fabricated using $(45°/-45°)_{3S}$ layup. Test samples were 2.54 cm wide and 22.86 cm long and were mounted with four 2.54 cm wide and 5.08 cm long fiberglass tabs. Open-hole tensile samples were laminated employing $(45/90/-45/0)_{2S}$ sequence. Test specimens were 3.81 cm wide and 22.86 cm long, and a hole 0.635 cm in diameter was drilled through the center of the flat specimens. The loading rate during testing was 0.127 cm/min.

RESULTS AND DISCUSSION

Tensile and flexural properties of LCP-CF composites are given in Tables II and III. The wet "conditions" in Tables II and III refer to samples immersed in water at 160°F for 2 weeks prior to testing at the indicated

TABLE IV
Shear Strength of LCP-Celion 6000 Composites

Fiber content (vol %)	Conditions	Shear strength MPa (ksi)
58	RT	52 (7.6)
58	200°F	37 (5.4)
58	250°F	23 (3.9)

TABLE V
Compression Properties of LCP-Celion 6000 Composites

Fiber content (vol %)	Conditions	Compression	
		Strength, MPa (Ksi)	Modulus, GPa (msi)
45	RT	809 (117.5)	117 (17)
50	RT	862 (125.0)	120 (17.5)

temperature. Both tensile and flexural properties are comparable to those of commercial epoxy-CF composites at the same fiber volume content. Flexural modulus retention at elevataed temperatures is extremely good. However, the flexural strength retention at 200°F is only fair (67%) and becomes poor (54%) at a test temperature of 250°F. This poor retention may be due to a poor interface between fiber and matrix. Thus, the adhesion between fibers and matrix fails long before the composites fails.

Table IV and V summarize the shear strength and compression properties of LCP-CF composites. Both shear and compression strengths are slightly inferior to those of the epoxy-carbon fiber composites but are in the range for the secondary composite applications. Compression samples failed through fiber buckling and composite delamination. Figures 10 and 11 show scanning electron micrographs (SEM) of the fracture surface of a tested compression sample. Fiber buckling and delamination surfaces are evident. Figure 10 clearly indicates that every fiber has been surrounded with matrix, but adhesion between them is poor. Figure 11 demonstrates that fibers have good alignment but poor interfacial adhesion. Therefore, the poor compression and shear strength may be attributed to poor interfacial adhesion between unsized carbon fiber and LCP matrix as well as poor intermolecular cohesion within the LCP polymer. The poor interfacial adhesion has also been confirmed by the poor interlaminar shear strength measured according to Boeing's specification.

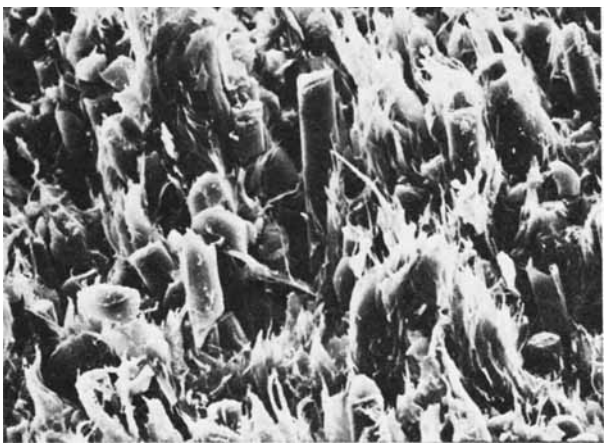

Fig. 10. Fracture surface of a compression sample (× 1000).

Fig. 11. Delamination surface of a compression surface (× 96).

The mechanical properties of an isotropic laminate are given in Table VI. Both open-hole and ± 45° tensile strength are comparable to those of epoxy-carbon fiber composites. Impact test results indicate that the isotropic panel has a maximum load of 2420 N, which is clearly superior to thermoset matrix systems (typically 1480 N).

CONCLUSIONS

The following conclusions can be drawn from this study. Due to the advantage of low melt viscosity of liquid-crystal polymers, LCP-CF composites with uniform fiber distribution, good wetout, and low void content have been easily developed using conventional pultrusion equipment.

A significant number of mechanical properties of LCP-CF composites are comparable to those of epoxy-CF composites. LCP-CF composites have superior impact resistance to thermosetting matrix counterpart. However, deficiencies in shear strength and compression strength are apparent. These deficiencies may be attributed to the poor interfacial adhesion between matrix and fiber and poor intermolecular adhesion within the LCP polymer.

The author wishes to acknowledge the financial support received from NASA-Langley Research Center (Contract NAS1-15479).

TABLE VI
Mechanical Properties of Isotropic Laminated Panel (LCP-Celion 6000)

Property	CF (vol %)	Result	
Open-hole tensile strength	52	313.5 MPa	(45.5 ksi)
45° tensile strength	53	134.5 MPa	(19.5 ksi)
Impact test:	52	2420 N	(740 lb)
Max. load			
Energy at max. load	52	2.76 J	(2.04 ft/lb)

References

1. J. T. Hoggatt, Investigation of Reinforced Thermoplastics for Naval Aircraft Structural Applications, contract N0001972-C0526 (1973).
2. G. Husman and J. Hartness, 24th Nat'l *SAMPE Symp.*, **24**(2), 21 (1979).
3. J. Hartness, 25th Nat's. *SAMPE Symp.*, **25**, 376 (1980).
4. J. Hartness, 14th Nat'l. *SAMPE Technical Conf.*, **14**, 26 (1982).
5. J. Hartness, *SAMPE Qu.*, 33, (1983).
6. P. E. McMahon and M. Maximovich, 3rd Internat'l. Conf. on Composite Mtls., Paris (1980).
7. C. H. Sheppard and E. E. House, Development of Improved Graphite Reinforced Thermoplastic Composites, contract N0001980-C-0365 (1981).
8. R. B. Rigby, 27th National *SAMPE Symp.*, **27**, 747 (1982).
9. G. R. Belbin, I. Brewster, F. N. Cogswell, D. J. Hezzell, and M. S. Swerdlow, 2nd Intercontinental *SAMPE Conf.*, Stresa, Italy (1982).
10. J. Hartness and R. Y. Kim, 28th Nat'l *SAMPE Symp.*, **28**, 535 (1983).
11. F. N. Cogswell, 28th Nat'l. *SAMPE Symp.*, **28**, 528 (1983).
12. H. F. Kuhfuss and W. J., Jackson, Jr., U.S. patent No. 3,778,410 (Dec. 11, 1973).
13. Idem, U.S. Patent No. 3,804,805 (Apr. 16, 1974).
14. J. R. Jackson, Jr., and H. F. Kuhfuss, *J. Polym. Sci., Polym. Chem. Ed.*, **14**, 2043 (1976).
15. T. C Pletcher, U.S. Patent Nos. 3,991,013 and 3,991,014 (Nov. 9, 1976).
16. J. R. Schaefgen, U.S. Patent No. 4,075,262 (Feb. 21, 1978).
17. J. R. Schaefgen, U.S. Patent No. 4,118,372 (Oct. 3, 1978).
18. R. S. Irwin, U.S. Patent No. 4,176,223 (Nov. 27, 1979).
19. W. J. Jackson, Jr., and H. F. Kuhfuss, U.S. Patent No. 4,140,846 (Feb. 20, 1979).
20. W. J. Jackson, Jr., and J. C. Morris, U.S. Patent No. 4,181,792 (Jan. 1, 1980).
21. G. W. Calundann, U.S. Patent No. 4,130,545 (Dec. 19, 1978).
22. G. W. Calundan, U.S. Patent No. 4,161470 (Jul. 17, 1979) and U.S. Patent No. 4,184,996 (Jan. 22, 1980).
23. S. Baxter and A. B. D. Cassie, *J. Text. Inst.*, T67 (1945).
24. G. W. Smith, in *Advances in Liquid Crystals*, Vol. 1, G. H. Brown, Ed., Academic, N. Y. 1975, p. 189.
25. White and Fellers, *J. Appl. Polym. Sci., Symp.*, **33**, 137 (1978).
26. J. I. Jin, S. Antoun, C. Ober, and R. W. Lenz, *Brit. Polym. J.*, **Dec**, 133 (1980).
27. C. Ober, R. W. Lenz, G. Galli, and E. Chiellini, *Macromolecules*, **16**, 1034 (1983).
28. W. J. Jackson, Jr., *Macromolecules*, **16**, 1027 (1983).
19. W. R. Kirgbaum, J. Watanable, and T. Ishikawa, *Macromolecules*, **16**, 1271 (1983).
30. G. W. Calundann and M. Jaffee, Anisotropic Polymers, Their Synthesis and Properties, Proceedings of the Robert A. Welch Foundation Conferences on Chemical Research, Research Conference XXVI, Synthetic Polymers (1982).
31. R. S. Porter and J. F. Johnson, in *Rheology*, Vol. 4, F. R. Eirich, Ed., Academic, New York, Chapter 5, (1967), p. 317.
32. D. G. Baird, in *Advances in Liquid Crystals*, Vol. 4, G. H. Brown, Ed., Academic New York, 1979.
33. K. F. Wissbrun, *J. Rheol.*, **25**, 619 (1981).
34. S. Onogi and T. Asada, in *Rheology*, Vol. 2, G. Astarita, G. Marrucci, and L. Nicolais, Eds., Plenum, New York, 1980.
35. G. Kiss and R. S. Porter, *J. Polym. Sci., Polym. Phys. Ed.*, **18**, 361 (1980).
36. G. Kiss and R. S. porter, *J. Polym. Sci, Polym. Phys. Ed.*, **65**, 193-211 (1978).
37. K. F. Wissbrun, *Brit. Polym. J.*, **Dec.**, 163, (1980).
38. K. F. Wissbrun and A. C. Griffin, *J. Polym. Sci., Phys. Ed.*, **20**, 1835 (1982).
39. A. J. East, L. F. Charbonneau, and G. W. Calundann, U.S. Patent No. 4,330,457.
40. A. J. Kinlock, S. J. Shaw, D. A. Tod, and D. L. Hunston, *Polymer*, **24**, 1341 (1983).
41. T. S. Chung, Liquid Crystal Polyester-Carbon Fiber Composites, NASA Contract Report No. 172323 (1984).

Received March 19, 1985
Accepted May 6, 1985